2D ^{31}P Exchange NMR: A new Approach for a Direct Probing of the Connectivities of Q^n Units in Glasses

R. Born, M. Feike, C. Jäger, and H. W. Spiess

Max-Planck-Institut für Polymerforschung, Postfach 31 48, D-55021 Mainz, Germany

Z. Naturforsch. **50a**, 169–176 (1995); received September 26, 1994

Dedicated to Prof. W. Müller-Warmuth on the occassion of his 65th birthday

Recently, ^{31}P two-dimensional (2D) NMR has been proposed as a powerful tool for direct investigations of the connectivities between the Q^n units in glasses, i.e. the medium-range order. In this paper, the principles of these experiments and applications to both polycrystalline $Mg_2P_2O_7$ and a Na_2O–P_2O_5 glass are demonstrated, including a theoretical description and modelling of the polarization transfer between the two inequivalent phosphorus sites in the magnesium pyrophosphate.

Key words: Exchange NMR, Connectivities, Phosphate glasses, Dipolar coupling, MAS

1. Introduction

NMR is a powerful tool for structural investigations of glasses and other disordered solids. In particular ^{29}Si and ^{31}P MAS NMR (MAS: Magic Angle Spinning) provide the opportunity to determine the distributions of silicon and phosphorus over the various Q^n units (n: number of bridging oxygen atoms between like SiO_4 or PO_4 units [1]) forming the network of a glass. One-dimensional (1D) MAS NMR has been applied to a variety of different glass systems and ceramics in order to investigate e.g. the influence of different sorts of cations on the micro structure of the material or to check the applicability of the binary or random modified network models of the distributions of the Q^n groups [2–8].

However, despite the success of such 1D NMR investigations for the structural analysis of amorphous materials, they cannot yield direct information about the medium range order in such solids, especially about the connectivity scheme between the various Q^n groups in the network. On the other hand, two-dimensional (2D) Exchange NMR [9] can yield such information directly and quantitatively. It is based on the same principle as the 2D nuclear Overhauser techniques employed for structural elucidation in biopolymers [9], where different structural units are identified by their chemical shifts, whereas their proximity is probed by magnetization exchange mediated by the dipole-dipole coupling.

The experimental details of the 2D Exchange NMR experiments are described in detail in Section 2. The procedure for describing the magnetisation transfer in two spin-systems with both anisotropic chemical shift effects and dipolar broadening is briefly outlined in Section 3. Experimental and theoretical results for $Mg_2P_2O_7$ are compared in Section 4. Finally, an application of this technique for probing the connectivity scheme in 36 mole% Na_2O–64 mole% P_2O_5 glass is shown (Section 5).

2. Experimental Details

Two Dimensional Experiments

In order to prove connectivities directly by NMR one has to establish a magnetisation transfer between the phosphorus nuclei in adjacent (directly bonded) PO_4 units. This can be achieved using either the J-coupling or the dipolar coupling between the nuclei. Multidimensional NMR experiments using the J-coupling are commonplace of the art in liquid state NMR [9]. However, in solid state NMR only few examples have been published so far for ^{29}Si NMR of inorganic materials such as zeolites and glasses [10–12]. For nuclei with high natural abundance (e.g. ^{31}P) it is much easier to exploit the dipole-dipole coupling. For phosphorus in a P-O-P moiety the dipolar broaden-

Reprint requests to Dr. C. Jäger.

0932-0784 / 95 / 0200-0169 $ 06.00 © – Verlag der Zeitschrift für Naturforschung, D-72027 Tübingen

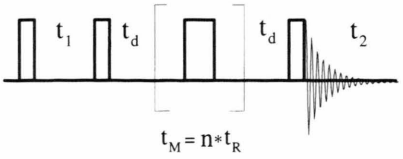

Fig. 1. 2D Exchange NMR pulse sequence used for the experiments. High speed MAS is applied throughout the entire experiment. The narrow rectangles denote 90° pulses whereas in the mixing time rotor synchronized 180° pulses (double sized rectangles) are applied for recoupling of the dipolar interaction. The delays t_d before and after the mixing time are inserted to destroy transverse magnetization and were chosen to be 50 ms.

ing can be estimated to about 1 kHz in a powder, compared with some ten Hertz or even less for the *J*-coupling of such bonds.

The pulse sequence is essentially the same as for 2D Exchange NMR widely applied in liquid and solid state NMR [9, 13] and is shown in Figure 1. Throughout the experiment high-speed MAS is applied. This ensures high resolution NMR spectra both in the ω_1 and ω_2 dimensions of the 2D NMR spectrum. Since MAS averages out the dipolar interaction, it must be recoupled during the mixing period t_m to ensure the necessary magnetization transfer. It should be noted that this magnetization transfer by spin diffusion is different from physical exchange which is associated with material transport. There are several approaches [e.g. 14–18] to achieve the recoupling. We have chosen a rotor synchronized irradiation of one 180° pulse in the middle of a single rotor period [14] which has been shown to be an efficient method for recoupling of the homonuclear dipolar coupling between the phosphorus nuclei. The 90° pulse length was 2.2 μs and a repetition time of 50 s has been used. The sample was spun at 12.5 kHz. Time proportional phase incrementation (TPPI) with phase cycling has been applied to obtain pure absorption mode spectra [9]. The resonance frequency was 121.5 MHz. 4, 16 and 32 scans per t_1 increment have been acquired for the spectra with 0 ms, 2.5 ms and 10 ms mixing time, respectively. 1000, 280, and 50 t_1 increments with 25 μs incrementation time have been acquired for the three experiments with the different mixing times.

One Dimensional Experiments

The 2D NMR experiments are quite time consuming. Thus, for the investigation of the time dependence

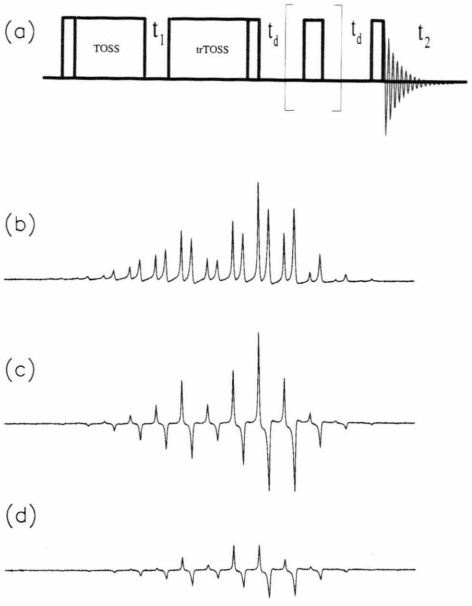

Fig. 2. The TIPSY sequence consists of a TOSS sequence, followed by a delay and a time reversed TOSS sequence (a). The delays t_d have been inserted to allow the dephasing of unwanted magnetization. TIPSY can be used to generate a non-equilibrium starting magnetization, if only two lines are present. One side-band pattern of the regular spectrum (b) can be inverted (c). Under the influence of the recoupling sequence, the difference magnetization decreases (d). We monitor the difference of the intensities of the two side band patterns. For clarity spectra with a spinning speed of 2000 Hz are presented, whereas the actual experiments have been carried out at 8000 Hz.

of the magnetization exchange of a model compound ($Mg_2P_2O_7$), we have used a suitable 1D version of the experiment (Figure 2). Due to the inequivalence of the two phosphorus sites, the ^{31}P spectrum displays two separated lines. One of these lines can be inverted to create a non equilibrium start magnetization $I_{z1} - I_{z2}$. To achieve this, we use the TIPSY sequence of Geen, Levitt, and Bodenhausen [19]. After the creation of the initial state and a suitably selected delay for the dephasing of unwanted transverse magnetization we irradiate the recoupling sequence during the mixing time t_m. Under the influence of the reintroduced dipolar coupling, the system equilibrates and $\langle I_{z1} - I_{z2} \rangle$ smoothly decays from its starting values. For long times t_m the difference magnetization should vanish. After the irradiation of the recoupling sequence for a time t_m we record the resulting magnetization (readout 90° pulse). By integrating the intensity of the two peaks, we get $\langle I_{z1} \rangle, \langle I_{z2} \rangle$ and hence $\langle I_{z1} - I_{z2} \rangle$ as

function of t_m. The parameters for these 1 D experiments are: spinning speed 8000 Hz, 90° pulse length 1.7 μ sec, 180° pulse length 3.0 μ sec, the TOSS separations are those of the 6 pulse TOSS experiment [20], the delay separating TOSS and trTOSS in TIPSY $t_1 = 657$ μ sec, dephasing delay $t_d = 10$ msec. The sample was doped with 0.2% Fe^{3+} to allow for a relatively short repetition time of 10 sec.

3. Theoretical Modeling of the Magnetization Transfer

From a theoretical standpoint, we have to consider a system of two like spin-1/2 nuclei I_1 and I_2 which are subject to both the homonuclear dipolar coupling and anisotropic chemical shifts. Additionally, one rotor synchronized 180° pulse per rotor period is irradiated for the recoupling of the homonuclear dipole interaction as explained earlier. This has to be taken into account in order to calculate the magnetization transfer (longitudinal order I_z) from one nucleus (e.g. I_1) to the other (I_2).

Neglecting the recoupling pulses, the theory is very similar to the treatment of rotational resonance [21]. The interaction Hamiltonian is

$$H = \omega_1 I_{z1} + \omega_2 I_{z2} + \omega_D (3 I_{z1} I_{z2} - \boldsymbol{I}_1 \cdot \boldsymbol{I}_2).$$

As a result of magic angle sample spinning, the interaction parameters ω_1, ω_2 (both represent the chemical shifts) and ω_D (dipolar coupling) become time-dependent, e.g.,

$$\omega_1(t) = \omega_1^{iso} + \tfrac{1}{2}\delta_1\gamma((3\cos^2\vartheta_1(t) - 1) - \eta_1 \sin^2\vartheta_1(t)\cos 2\phi_1(t)).$$

The explicit time dependence of these terms can be obtained by transforming the principal axis system (PAS) of both the chemical shift tensor and the dipolar tensor into the laboratory frame. This is done by successive application of Euler rotations from the principal axis system to the molecular system (MF), the rotor system (RF) and finally to the laboratory frame (LF):

$$\text{PAS} \longrightarrow \text{MF} \xrightarrow{(\alpha\beta\gamma)} \text{RF} \xrightarrow{(\omega_r t, \Theta_m, 0)} \text{LF}.$$

In the second transformation, the statistical orientation of the crystallites (α, β, γ) in a powder has to be included. The last transformation represents the mechanical rotation of the sample with angular frequency ω_r about the magic angle Θ_m. The explicit expressions for $\omega_1(t)$, $\omega_2(t)$ and $\omega_D(t)$ can be found in the literature [21].

The Hamiltonian may be split into two parts

$$H = H_1 + H_2,$$
$$H_1 = \tfrac{1}{2}(\omega_1 + \omega_2)(I_{z1} + I_{z2}) + 2\omega_D I_{z1} I_{z2},$$
$$H_2 = \tfrac{1}{2}(\omega_1 - \omega_2)(I_{z1} + I_{z2}) - \omega_D(I_{x1} I_{x2} + I_{y1} I_{y2}).$$

Only for an isolated two-spin system of spin-1/2 nuclei the Hamiltonians H_1 and H_2 commute. If we use the states $|1\rangle = |++\rangle$, $|2\rangle = |-+\rangle$, $|3\rangle = |-+\rangle$, $|4\rangle = |--\rangle$, the Hamiltonians are in matrix representation

$$H_1 = \frac{1}{2}\begin{vmatrix} \omega_1+\omega_2+\omega_D & 0 & 0 & 0 \\ 0 & -\omega_D & 0 & 0 \\ 0 & 0 & -\omega_D & 0 \\ 0 & 0 & 0 & -\omega_1-\omega_2+\omega_D \end{vmatrix},$$

$$H_2 = \frac{1}{2}\begin{vmatrix} 0 & 0 & 0 & 0 \\ 0 & \omega_1-\omega_2 & -\omega_D & 0 \\ 0 & -\omega_D & -\omega_1+\omega_2 & 0 \\ 0 & 0 & 0 & 0 \end{vmatrix}.$$

Magnetization exchange between the two nuclei may then be monitored as a transition between the coherences $|2\rangle\langle 2|$ and $|3\rangle\langle 3|$. This exchange is produced by H_2 alone, since only this Hamiltonian contains the important "flip-flop"-term $I_{x1} I_{x2} + I_{y1} I_{y2}$. As the Hamiltonians commute, the time evolution operator can be decomposed:

$$U(t_b, t_a) = U_1(t_b, t_a)\, U_2(t_b, t_a),$$
$$U_1(t_b, t_a) = \exp\left[-i \int_{t_a}^{t_b} H_1(t')\,dt'\right],$$
$$U_2(t_b, t_a) = T\exp\left[-i \int_{t_a}^{t_b} H_2(t')\,dt'\right].$$

T is the Dyson time ordering operator. The density matrix evolves under the propagator according to

$$\varrho(t) = U(t, 0)\,\varrho(0)\,U^*(t, 0),$$

where $\varrho(0)$ is the initial state. For the 1 D experiments, this initial state is $I_{z1} - I_{z2}$. The propagator of the diagonal Hamiltonian H_1 does not pose any problem. But H_2 is homogeneous, i.e. $H_2(t)$ and $H_2(t')$ do not commute for $t \neq t'$ in general. Thus, U_2 must be calculated numerically. The effects of the r.f. pulses can be

considered by applying the transformation

$$|1\rangle \rightarrow -\exp(+2i\varphi)|4\rangle,$$
$$|2\rangle \rightarrow -|3\rangle,$$
$$|3\rangle \rightarrow -|2\rangle,$$
$$|4\rangle \rightarrow -\exp(-2i\varphi)|1\rangle$$

for an ideal 180°-pulse with phase φ.

The numerical evaluation of U_2 is done by transforming the problem into Liouville space. The zero-quantum coherences $|2\rangle\langle 3|$ and $|3\rangle\langle 2|$ are subject to relaxation, which may be incorporated by introducing a relaxation rate $1/T_{2,\mathrm{ZQ}}$ for these terms. The value of the parameter $T_{2,\mathrm{ZQ}}$ is not easily obtained by experiment and is a free parameter in our simulation. The time ordering in U_2 can be avoided by splitting a rotor period into 50 small intervals where the Hamiltonian is assumed to be constant. The evaluation of the propagator for such a small time interval $(t, t+\Delta t)$,

$$U(t+\Delta t, t) \approx \exp[-i\Delta t H_2(t)],$$

is done by diagonalization of $H_2(t)$ in Liouville space. After each rotor period the magnetization exchange is calculated via

$$\Delta M_z(t) = \mathrm{Tr}[\varrho(t)(I_{z1} - I_{z2})].$$

This has to be done for every orientation (α, β, γ) for the molecular frame. The powder average is performed by the random generation of several thousand orientations and subsequent addition of the magnetization exchange curves of all crystallites.

The procedure involves some complex algebra and was encoded in FORTRAN-77 and the IMSL numerical subroutines were used for matrix operations. All of the simulations were done on a DEC/VAXStation 3200. One calculation for a single set of parameters and 2000 different crystallite orientations takes about one hour.

The magnetization exchange curve depends on the following parameters:

1) The principal values of the chemical shift tensor,
2) the orientation of the chemical shift tensors with respect to the molecular frame,
3) the distance of the nuclei and thus the dipolar coupling,
4) the orientation of the dipolar tensor in the molecular system,
5) The zero quantum relaxation time $T_{2,\mathrm{ZQ}}$,
6) The B_0-field and 7) the spinning speed ω_r.

4. $Mg_2P_2O_7$ – a model compound

Magnesium pyrophosphate has two inequivalent phosphorus sites (Figure 3). It has already been extensively studied by various methods [22, 23] and is therefore a suitable model compound to elucidate the nature and parameter dependence of the magnetization exchange. It is, moreover, a classical two spin system which permits the easy comparison of experimental results with simulated data. The essential parameters are listed below in Table 1.

Even in amorphous systems, principal tensor components of the shift tensors can be obtained by various experimental methods. But tensor orientations and intermolecular distances are much more difficult to determine. Therefore, we focus on the influence of these parameters on the exchange curve. Figure 4 shows the difference magnetization $\langle I_{z1} - I_{z2}\rangle$ as a function of t_m for various P-P interatomic distances. The other parameters were kept fixed and set to values that yield a good agreement with experimental data, if the correct interaction distance is chosen (vide infra). We find a strong dependence of the exchange rate on the interatomic distance d. For $d = 1$ nm, there is virtually no exchange. Thus, the technique probes the local environment of the nucleus. The magnetization transfer should be restricted to the nearest and perhaps to a considerably lesser degree to next nearest phosphorus neighbours. The efficiency of the magnetization exchange is also strongly dependent on the

Space group	$B2_1/c$
P–P distance	0.302 nm
P_1, σ_{iso}	−20.3 ppm
$\Delta\sigma$	128 ppm
η	0.38
P_2, σ_{iso}	−14.0 ppm
$\Delta\sigma$	98 ppm
η	0.08

Table 1. Important parameters for $\alpha - Mg_2P_2O_7$.

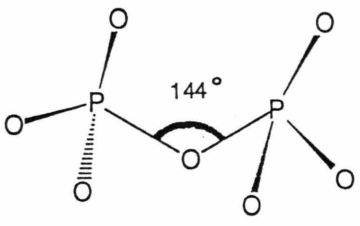

Fig. 3. Schematic drawing of the $[P_2O_7]^{4-}$ anion. The P–O–P bond angle is taken from [23].

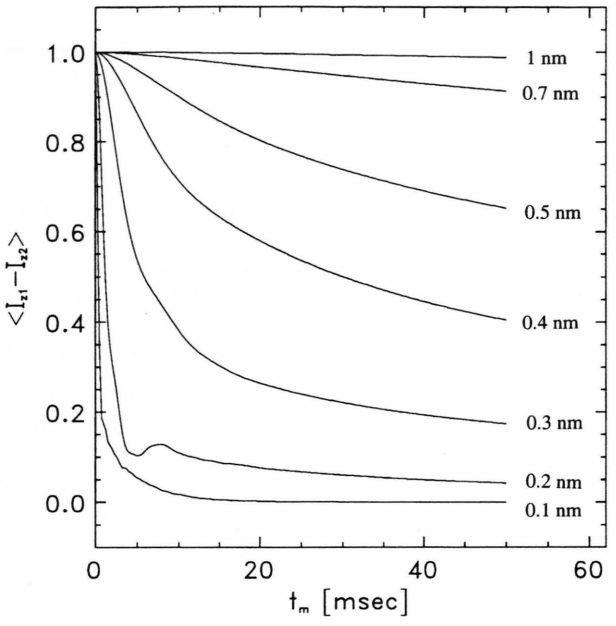

Fig. 4. Difference magnetization $\langle I_{z1} - I_{z2}\rangle$ as a function of the mixing time t_m for various P–P interatomic distances. The chemical shift parameters for the simulation have been taken form [22]. Due to the $1/r^3$ dependence of the dipolar interaction the magnetization exchange is effective only for small distances.

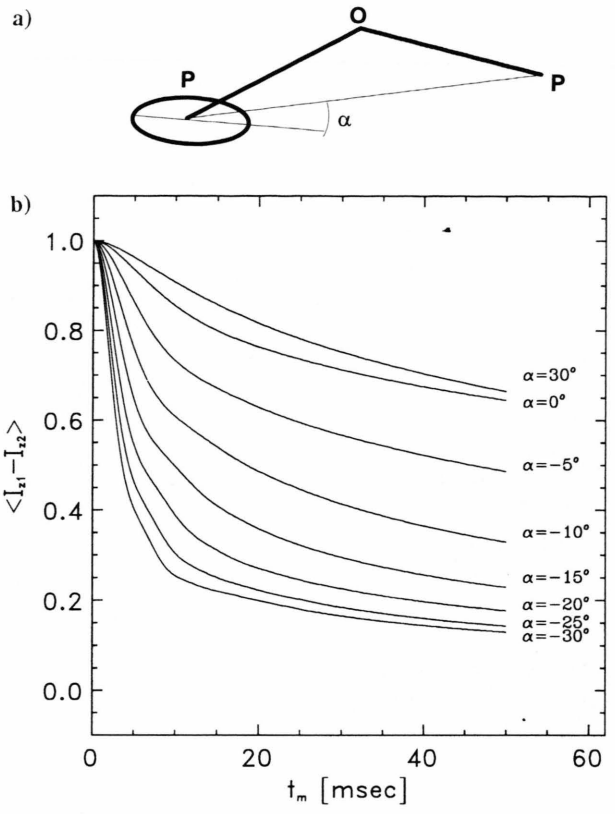

Fig. 5. The orientation of the chemical shift tensor with respect to the molecular frame is another parameter of the simulation. The angle α denotes the deviation of the tensor z-axis from the P–P interatomic vector (a). Small variations of α have a great impact on the magnetization exchange curve (b).

tensor orientation (Figure 5). Variations as small as 5° have an astonishing impact on the exchange rate. The best agreement with experiment is achieved, if the z-axes of the chemical shift tensors are oriented almost parallel to the P–O-bond (Fig. 6), while the other parameters are set to the values given in the table. A zero quantum relaxation time of $T_{2,ZQ} = 3$ msec is assumed. This orientation is suggested by physical intuition as well. The remaining deviations of experimental data and simulation results are due to experimental uncertainties and the influence of remote nuclei, which disturb the two-spin system of a single pyrophosphate ion. For longer mixing times t_m, longitudinal relaxation must be taken into account.

Thus, reasonable agreement of experiment and simulation can be achieved for the simple model compound $Mg_2P_2O_7$. As a matter of completeness it should be mentioned that the equivalent information on relative shielding tensor orientations and atomic distances for isolated spin pairs such as in $Mg_2P_2O_7$ may also be obtained by slow speed spinning. This approach has been described in detail in the literature [24].

In our view the sensitivity of the exchange curve to interatomic distances and tensor orientation can be used to elucidate the distance and tensor orientation distribution function of phosphate glasses as well.

5. Application of 2D NMR to a Na_2O-P_2O_5 glass

Recently the very first application of 2D Exchange NMR for probing the connectivity scheme in phosphate glasses was presented [25].

Figure 7 shows the contour plots of the 2D Exchange NMR spectra (centre band region) for three different mixing times (a) $t = 0$ ms, b) $t = 2.5$ ms and c) $t = 10$ ms. Most interesting is the important fact, that for zero mixing time (hence no magnetization transfer among the Q^n units) an extremely narrow diagonal

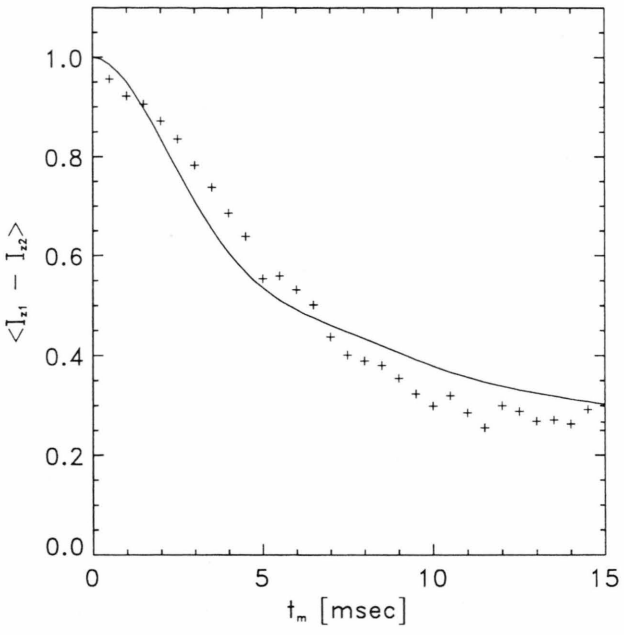

Fig. 6. Comparison of experimental (+) and theoretical (full line) exchange curve. The agreement is reasonable, if the z-axes of the shift tensors are aligned almost parallel to the P–O bonds ($\alpha_1 = 20°$, $\alpha_2 = 16°$).

spectrum is found. This clearly demonstrates that the inhomogeneous line broadening is due to a distribution of the isotropic chemical shifts. The homogeneous broadening can be estimated from the perpendicular width of the diagonal spectrum (ca. 1 ppm). Actually, it is governed by the maximum t_1 value which was "only" incremented up to 25 ms (1000 increments!). An independent Carr-Purcell-Meiboom-Gill experiment [26] yielded a homogeneous line width of less than about 0.3 ppm. In other words, the homogeneous line broadening is negligible in such phosphate glasses under high-speed MAS conditions and the broadening is solely inhomogeneous. Hence, any

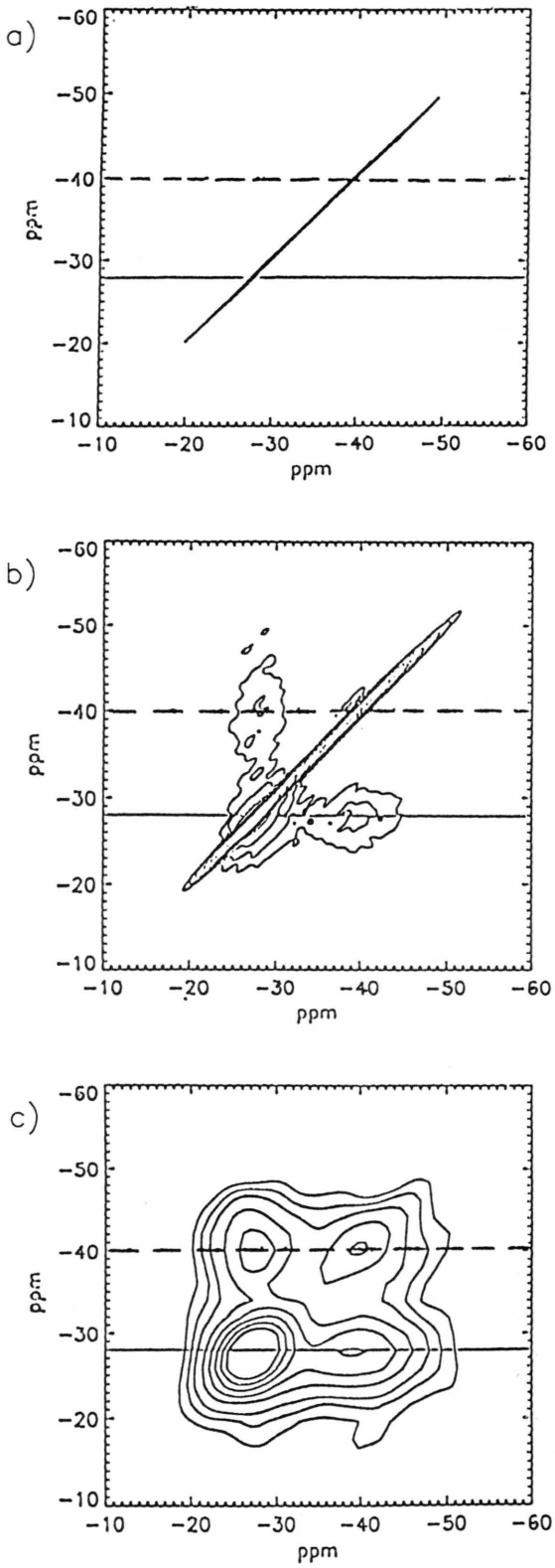

Fig. 7. Contour plots of the 2D Exchange NMR spectra (center band region only) for $t_m = 0$ ms (a), $t_m = 2.5$ ms (b), and $t_m = 10$ ms (c). The interpretation of the 2D spectrum for $t = 2.5$ ms implies connectivities among Q^2 and Q^3 units or vice versa, but direct linking between like units can almost be excluded. This conclusion is primarily based on the fact, that the diagonal is much narrower than the cross peaks (see also cross-sections in Figure 8). However, for longer mixing times (Fig. 7c) the diagonal also broadens and the cross-section through the Q^2 peak is equivalent to the projection (see also Fig. 8 and text). The position of the cross sections for the Q^2 (full line) and Q^3 (dashed) groups is indicated.

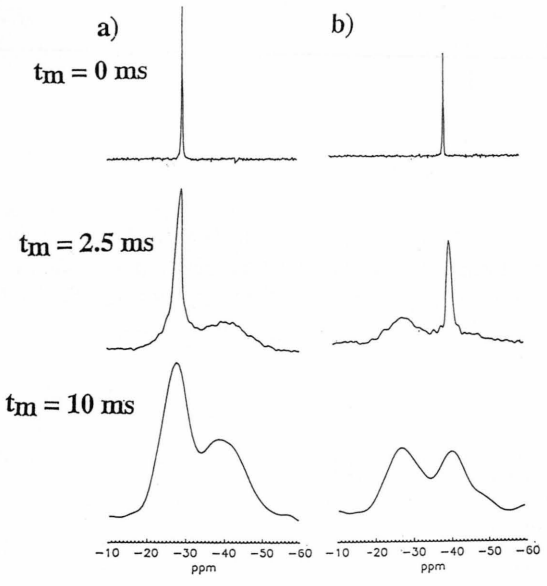

Fig. 8. Cross sections taken through the Q^2 (a) and Q^3 (b) areas for the three various mixing times. For details see text.

off-diagonal intensity in the 2D spectrum due to magnetization exchange in the mixing period is a direct indication of connectivities in the amorphous network. Because of the extremely small homogeneous line width, we explicitly note, that connectivities not only between different Q^n groups can be detected, but also among like units, e.g. among Q^2 or among Q^3 which differ in their chemical shifts. This feature means detection of medium range order in a direct manner which is the main objective of our investigations. It requires purely absorptive 2D NMR data acquisition and data processing.

For both non-zero mixing times (Fig. 7b and 7c) considerable off-diagonal intensity is observed. The 2D exchange NMR spectrum for $t_m = 2.5$ ms is most interesting, since this is approximately the time necessary for a magnetization transfer among adjacent PO_4 units. The broad cross peaks confirm the linking of the Q^2 and Q^3 units in the glass. But even more important, the diagonal is still much narrower than the Q^2-Q^3 exchange peaks for this mixing time. For even longer mixing times (10 ms in Fig. 7c) the diagonal is also broadened clearly proving the magnetization transfer both among like and different Q^n units.

These experimental results can be discussed more conveniently in terms of the connectivity scheme of that glass using the various cross sections taken through the Q^2 and Q^3 peaks (Figure 8). The reason is that all the cross sections yield information on the connectivity whenever either cross peaks appear or linebroadening of the diagonal is observed. For zero mixing time, of course, very sharp cross sections are found for both the Q^2 (Fig. 8a) and Q^3 (Fig. 8b) units as described earlier. For 2.5 ms mixing time (which is approximately the time for a magnetization transfer between adjacent units), no exchange intensity is found within the Q^3 unit region at about -40 ppm and only little in the Q^2 area. This can be infered from the small but broad foot in the Q^2 cross section in addition to the still narrow diagonal Q^2 spectrum, as well as the Q^2-Q^3 cross peaks. On the other hand, for 10 ms mixing time, both a substantial increase of the cross-peak intensities and a broadening of the diagonal are detected in the Q^2 and Q^3 cross sections. In fact the cross-section through the Q^2 peak is now almost equivalent to the projection of the entire 2D spectrum and the 1D spectrum [25]. This means that a complete magnetization exchange has already taken place after 10 ms. Hence, these two 2D Exchange NMR spectra with mixing times of 2.5 ms and 10 ms suggest an almost regular connectivity scheme with an alternating sequence of Q^2 and Q^3 units in this glass as sketched in Figure 2. In addition this some of the Q^2 units are also linked with like units but to a minor extent, which agrees with the glass composition.

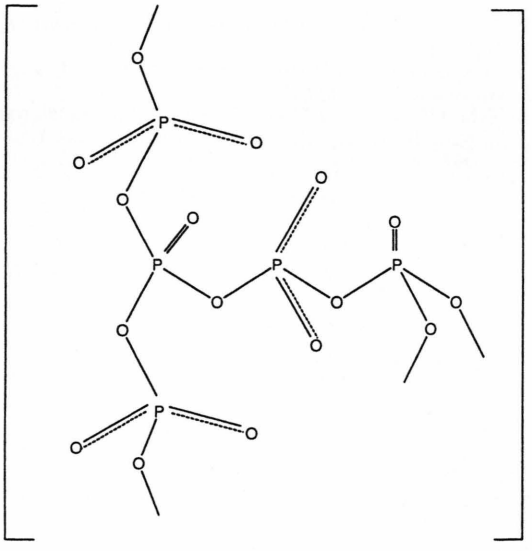

Fig. 9. Suggested structure for the phosphate glass. There is an almost regular alternating sequence of Q^2 and Q^3 units. Links among Q^2 units are not that important.

6. Conclusion

In summary, 2D homonuclear Exchange NMR can easily be applied to glasses for refined microstructural investigations exploiting the dipolar coupling between the nuclei. We propose it as a sensitive and unique method to study medium range order and even long range order in glasses in a direct fashion not requiring models or assumptions. For a detailed quantitative analysis of the exchange peaks in terms of the connectivity scheme theoretical modelling is essential. We have presented here the first results on the way towards a better understanding of the nature of amorphous solids.

Acknowledgements

C. J. and M. F. would like to thank the Deutsche Forschungsgemeinschaft for financial support. We are grateful to Dr. D. Sprenger for preparing the well defined glass used for these investigations.

[1] G. Engelhard and D. Michel, High-resolution solid-state NMR of silicates and zeolites, John Wiley, Chichester 1987.
[2] H. Eckert, Progr. NMR Spectr. **24,** 159 (1992).
[3] R. Dupree, D. Holland, and M. G. Mortuza, J. Non-Cryst. Solids **116,** 148 (1990).
[4] H. Maekawa, T. Maekawa, K. Kawamura, and T. Yokokawa, J. Non-Cryst. Solids **127,** 53 (1991).
[5] W. Hater, W. Müller-Warmuth, M. Meier, and G. H. Frischat, J. Non-Cryst. Solids **113,** 210 (1989).
[6] J. Stebbins, J. Non-Cryst. Solids **106,** 359 (1988).
[7] A. R. Grimmer, M. Mägi, M. Hähnert, H. Stade, A. Samoson, W. Wieker, and E. Lippmaa, Phys. Chem. Glasses **25,** 105 (1984),
[8] P. Losso, B. Schnabel, C. Jäger, U. Sternberg, D. Stachel, and D. O. Smith, J. Non-Cryst. Solids **143,** 265 (1992).
[9] R. R. Ernst, G. Bodenhausen, and A. Wokaun, Principles of Magnetic Resonance in One and Two Dimensions, Clarendon Press, London 1990.
[10] C. A. Fyfe, H. Gies, and Y. Feng, J. Amer. Chem. Soc. **111,** 7702 (1989).
[11] W. Kolodziejski and J. Klinowski, Solid State NMR **1,** 41 (1992).
[12] CTG Knight, R. J. Kirkpatrick, and E. Oldfield, J. Non-Cryst. Solids **116,** 140 (1990).
[13] K. Schmidt-Rohr and H. W. Spiess, Multidimensional Solid State NMR and Polymers, Academic Press, London 1994.
[14] A. E. Benett, J. H. Ok, R. G. Griffin, and S. Vega, J. Chem. Phys. **96,** 8624 (1992).
[15] J. H. Ok, R. G. S. Spencer, A. E. Benett, and R. G. Griffin, Chem. Phys. Lett. **197,** 389 (1992).
[16] R. Tycko and G. Dabbagh, Chem. Phys. Lett. **173,** 401 (1990).
[17] D. K. Sodickson, M. H. Levitt, S. Vega, and R. G. Griffin, J. Chem. Phys. **98,** 6742 (1993).
[18] T. Guillion and S. Vega, Chem. Phys. Lett. **194,** 423 (1992).
[19] H. Geen and G. Bodenhausen, J. Chem. Phys. **97,** 2928 (1992); H. Geen, M. H. Levitt, and G. Bodenhausen, Chem. Phys. Lett **200,** 350 (1992).
[20] D. P. Raleigh, E. T. Olejniczak, S. Vega, and R. G. Griffin, J. Magn. Res. **72,** 238 (1987).
[21] M. H. Levitt, D. P. Raleigh, F. Creuzet, and R. G. Griffin, J. Chem. Phys. **92,** 6347 (1990).
[22] U. Haubenreisser, Diss. B. Univ. Jena 1985.
[23] C. Calvo, Acta Cryst. **23,** 289 (1967).
[24] A. Kubo and C. A. McDowell, J. Chem. Phys. **92,** 7156 (1990).
[25] C. Jäger, M. Feike, R. Born, and H. W. Spiess, J. Non-Cryst. Solids **180,** 91 (1994).
[26] S. Meiboom and D. Gill, Rev. Sci. Instrum. **29,** 688 (1958).